DOI: 10.1002/ejic.200501023

Ten-Coordinate Neodymium(III) Complexes with Triethylenetetraaminehexaacetic Acid

Anna Mondry*[a] and Przemysław Starynowicz[a]

Dedicated to our teacher and friend Professor Krystyna Bukietyńska

Keywords: Chelates / Lanthanides / N ligands / Neodymium / UV/Vis spectroscopy

The crystal structures and spectroscopic (IR, Raman, UV/Vis) data for the complexes $[C(NH_2)_3]_2[Nd(HTTHA)]\cdot 3H_2O$ (**I**) and $[C(NH_2)_3]_3[Nd(TTHA)]\cdot 6H_2O$ (**II**) are presented. Crystals of **I** are triclinic, $P\bar{1}$, a = 9.998(2), b = 10.730(2), c = 15.557(3) Å, α = 106.89(3)°, β = 90.27(3)°, γ = 93.24(3)°, V = 1594.0(5) Å^3, Z = 2, while the chiral crystals of **II** are monoclinic, $P2_1$, a = 10.157(2), b = 15.958(3), c = 12.788(3) Å, β = 112.68(3)°, V = 1912.5(7) Å^3, Z = 2. Both structures consist of the complex monomeric anions, guanidinium cations and water of hydration. The Nd^{III} ions are ten-coordinate. The TTHA ligand coordinates to the Nd^{III} ions with six of its carboxyl oxygen atoms and four nitrogen atoms. Although the coordination environments of both Nd^{III} cations are essentially the same, the spectral results of both crystals reveal the influence of the degree of protonation of the ligand on the Nd^{III} ion. The IR and Raman spectra allowed us to assign some important frequencies. A comparison of the electronic absorption spectra of Nd^{III}–TTHA complexes in solution and in single crystals of **I** and **II** allows the detection of a small elongation of the Nd–O and Nd–N bonds in these complexes as compared to the $[Nd(TTHA)]^{3-}$ moiety in the previously reported complex $Na_3[Nd(TTHA)]\cdot 2.5NaClO_4\cdot 7.617H_2O$ and indicates that the coordination geometry of the ten-coordinate neodymium complex in solution is the same as in the chiral crystal **II**. The intensities of the f–f transitions in Nd^{III}–TTHA solutions and of crystals **I** and **II** were analysed on the basis of the Judd–Ofelt theory.

Introduction

The wide variety of biomedical applications of lanthanide complexes with polyamino polycarboxylic acids, including their use as contrast agents in MRI[1] and X-ray[2] diagnosis, NMR hyperfine shift-reagents[3] and bioanalytical assays,[4] is the reason for their being extensively investigated both in solution and in the solid state. The principal aim of these studies is to understand the physicochemical properties of these compounds in solution. In the case of lanthanide systems, one of the methods of choice is electron spectroscopy. Effective analysis of the spectroscopic data is, however, not a trivial task since the properties of these systems are dominated by the intraconfigurational f–f transitions, which are slightly influenced by the ligand field. Therefore, the results obtained by spectroscopic and electrochemical methods concerning the structure of complexes in aqueous solution are difficult to interpret. The situation is even more complicated in the case of lanthanide complexes with ligands characterised by a great number of functional groups, and tautomeric species of variously protonated donor groups of the ligand may be a reason that differently coordinated lanthanide species of diverse labilities coexist in solution. The lanthanide complexes with triethylenetetraaminehexaacetic acid (H_6TTHA), a ligand which has a sufficient number of donor atoms (six oxygen atoms and four nitrogen ones) to completely fill the first coordination sphere of the Ln^{III} ion, well exemplify the problems related to lanthanide species in solution. The absence of inner-sphere water molecules for Ln^{III}–TTHA solutions at pH above 3 has been proved by emission spectroscopy[5,6] as well as NMR studies,[7] and was also confirmed in the crystal structures.[8–16] Previously, the coexistence of two distinct complexes of Eu^{III}–TTHA in solution over the entire pH range has been reported.[5,17] This is different to the La^{III}–TTHA system, where the ^1H and ^{13}C NMR spectra revealed the existence of only one coordination arrangement around the metal cation in solution.[5] Our results based on the optical properties of Nd^{III},[8,16] Eu^{III}[17,18] and Ho^{III}[13] complexes with TTHA revealed that species differing in the number of coordinated nitrogen and oxygen atoms, namely $[Ln(N_4O_6)]^{3-}$/$[Ln(N_3O_6)]^{3-}$ and $[Ln(N_4O_5)]^{3-}$/$[Ln(N_3O_6)]^{3-}$, are present in the solution for the light and heavy lanthanide ions, respectively. Each of these species may form various stereoisomers, some of which may be op-

[a] Faculty of Chemistry, University of Wrocław,
Joliot-Curie 14, 50383 Wrocław, Poland
E-mail: anm@wchuwr.chem.uni.wroc.pl

tically active. Circularly polarized luminescence (CPL) spectroscopy following photoselective excitation has demonstrated the presence of the optically active enantiomers in a racemic mixture for the Eu^{III}–TTHA system.[19]

Although many structural relationships among Ln^{III}–TTHA complexes in solution are still unresolved, the spectroscopic results obtained for single crystals of these complexes are very helpful in understanding the background of the various processes that may occur in solution. Since the spectral properties of lanthanide complexes with TTHA in crystals, particularly those of Nd^{III}–TTHA crystals,[8,16] play an important role in determining the structure of $[Nd(TTHA)]^{3-}$ solution species, it seems advisable to examine the influence of the protonation degree and the countercation on the spectral properties of these complexes. In this paper we therefore report the crystal structures and UV/Vis spectroscopic data of crystalline guanidinium salts of the monoprotonated and deprotonated Nd^{III}–TTHA complexes in order to compare their spectral properties with the sodium salt of the Nd^{III}–TTHA complex in the crystal[8] and in aqueous solution at various pH values.

Results and Discussion

Crystal Structures

The crystal structures of $[C(NH_2)_3]_2[Nd(HTTHA)]\cdot 3H_2O$ (crystal **I**) and $[C(NH_2)_3]_3[Nd(TTHA)]\cdot 6H_2O$ (crystal **II**) were determined and it was found that **I** is isomorphic with $[C(NH_3)_2][La(HTTHA)]\cdot 3H_2O$.[9] The crystals of both compounds are composed of complex Nd^{III}–TTHA anions, guanidinium cations and water of crystallisation. As the TTHA anion is hexa-negative, a proton must be present in **I** to compensate the deficiency of the positive charge caused by the Nd^{III} ion and two guanidinium cations. The complex anions in both crystals are similar (Figure 1) and are composed of the TTHA residue wrapped around the neodymium cations. The metal ions are ten-coordinate, forming bonds with six carboxylic oxygen atoms and four nitrogen ones in each complex. The Nd–O and Nd–N bond lengths for **I** and **II** (Table 1) are typical and are similar to those found for the complex $Na_3[Nd(TTHA)]\cdot 2.5NaClO_4\cdot 7.617H_2O$,[8] denoted here as **Na1**. The differences between the positions of the atoms in both anions are most pronounced for the outer-sphere carboxylate oxygen atoms, which is most probably caused by different networks of hydrogen bonds. For example, the O(10) atom in **I** is involved in a short (2.67 Å) H-bond with a water molecule and a moderate bond with a guanidinium cation (O···N = 2.91 Å), whereas in **II** the O(10) atom forms three H-bonds of moderate lengths (2.87–3.08 Å) with two water molecules and a guanidinium cation. The proton that is necessary for the electric charge compensation in **I** is probably attached to O(12) as the C(17)–O(12) distance of 1.306(4) Å is about 0.05 Å longer than the other C–O bond lengths.

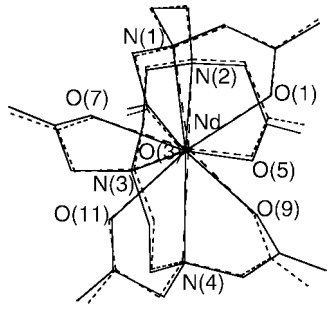

Figure 1. A view of the superimposed complex anions of **I** and **II**. The dashed lines represent **I** and the solid ones **II**. The atoms labels are given for the neodymium coordination sphere only, for the sake of clarity.

Spectral Results

IR and Raman Spectra of Crystals

A comparison of the IR and Raman spectra of **I** and **II** with the spectra of **Na1** and H_6TTHA allowed us to assign some important frequencies. These are given in Table 2. The IR bands of the three crystals **I**, **II** and **Na1**, in which the coordination environment (N_4O_6) around the Nd^{III} ion is the same, are displayed in Figure 2 (A). The vibrations of the OH and CH_2 groups, as well as of the NH_2 group in the case of the guanidinium crystals, occur in the broad and intense IR band located in the range 2750–3750 cm^{-1}. Since

Table 1. Selected bond lengths [Å] for Nd^{III}–TTHA crystals.

	$[C(NH_3)_2]_2[Nd(HTTHA)]\cdot 3H_2O$ **I**	$[C(NH_3)_2]_3[Nd(TTHA)]\cdot 6H_2O$ **II**	$Na_3[Nd(TTHA)]\cdot 2.5NaClO_4\cdot 7.617H_2O$[8] **Na1**
Nd–O(1)	2.448(3)	2.521(5)	2.537(3)
Nd–O(3)	2.492(3)	2.515(4)	2.491(4)
Nd–O(5)	2.418(3)	2.472(4)	2.434(4)
Nd–O(7)	2.435(2)	2.474(5)	2.430(3)
Nd–O(9)	2.439(3)	2.498(5)	2.521(3)
Nd–O(11)	2.801(3)	2.595(5)	2.524(4)
$Nd–O_{av}$	2.505	2.513	2.490
Nd–N(1)	2.774(3)	2.814(5)	2.742(4)
Nd–N(2)	2.764(3)	2.789(6)	2.763(4)
Nd–N(3)	2.720(2)	2.745(6)	2.724(4)
Nd–N(4)	2.853(3)	2.830(6)	2.823(4)
$Nd–N_{av}$	2.778	2.795	2.763
Nd–Nd	9.183(3)	10.157(3)	9.515(4)

combinations and/or overtones transitions may also appear in this spectral region, only the ν(OH) frequency of crystal water molecules can be unequivocally assigned. The positions of the ν(OH) peaks found in the three crystals may indicate that the overall strength of the hydrogen bond between water molecules and the polyatomic anion is the weakest in the case of **Na1** (Table 2). Broad bands of the $\nu(NH_2)$ mode were found in the Raman spectra of **I** and **II**. These vibrations, which are due to the guanidinium cation, appear in the range 3200–3400 cm^{-1}, where a combination band of the $\delta(NH_2)$ and $\nu_{as}(COO)$ overtones also appears. The positions of the $\nu(CH_2)$ oscillations in the IR spectra agree well with those very intense found in the Raman spectra. For both guanidinium crystals a strong band of the $\delta(NH_2)$ vibration was found in the region of 1650–1700 cm^{-1}. The $\nu_{as}(COO)$ frequencies of the studied crystals are very similar, with the highest frequency being found for **Na1**. The presence of a protonated carboxylate group in **I**, as the long Nd^{III}–O(11) distance attests (Table 1), is the reason for a much broader and split band of the $\nu_s(COO)$ vibration in **I** as compared with the bands of **II** and **Na1**.

The difference, Δ, between the antisymmetric and symmetric frequencies of the carboxylate groups has been suggested to be an indicator of the share of the M–O(COO) bond covalency,[20] the latter being higher when Δ increases. Accordingly, the Δ differences determined from the spectra of the three crystals were compared. Two values of Δ were found for the protonated crystal **I**. One of these differences was the highest one of all (200 cm^{-1}), while the second (187 cm^{-1}) is close to the Δ value of **Na1** (188 cm^{-1}). The smallest Δ was found for **II** (181 cm^{-1}). Comparing these Δ values with the structural data given in Table 1 one can see that they have no connection with the M–O bond lengths. A similar problem was encountered in the case of the Nd^{III}–N bond lengths, which may be reflected by the ν[C–$N(CH_2)$] modes. The smallest ν[C–$N(CH_2)$] frequency was found in the case of **I** (1116 cm^{-1}), whereas the ν(C–N) vibrations of **II** (1120 cm^{-1}) and **Na1** (1121 cm^{-1}) are similar to that of the ligand (1125 cm^{-1}). For both guanidinium crystals the most intense Raman bands of 1007 cm^{-1} were assigned to the ν[C–$N(NH_2)$] vibrations of the guanidinium cation. All ν(C–C) frequencies of the three crystals are blue-shifted relative to the frequency of the H_6TTHA ligand.

Although some similarity between the IR spectra of the crystals can be seen (Figure 2, **A**), one cannot say the same about their NIR spectra. These spectra, recorded at room temperature and 4 K, are shown in Figure 2 (**B**). Apart from the oscillation bands, the electronic $^4I_{9/2} \rightarrow {}^4I_{15/2}$ transition can also be observed in this region. Recently, we have shown that the f–f transitions in this spectral region are seriously affected by coincident combination and/or overtone bands.[21,22] The present data also reveal that these

Table 2. Wavenumbers [cm^{-1}] and relative intensities[a] of the bands observed in the IR and Raman spectra of H_6TTHA and crystals of **I**, **II** and **Na1**.

Tentative assignment	H_6TTHA IR	R	**I** IR	R	**II** IR	R	**Na1** IR
ν(OH)			3392 (s)		3411 (vs)		3438 (vs)
$\nu(NH_2)$[b]				3386 (m)		3369 (m)	
				3249 (m)		3242 (m)	
$\nu(CH_2)$	3026 (m)	3025 (m)					
	3019 (m)	3017 (m)	2986 (w)		2986 (w)		
	3006 (m)	3010 (m)	2970 (w)	2973 (vs)		2967 (s)	2955 (m)
	2995 (m)	2982 (s)		2946 (s)		2944 (s)	2923 (m)
	2966 (s)	2966 (vs)	2917 (w)	2901 (vs)	2890 (w)	2885 (s)	
		2934 (s)	2853 (w)	2851 (s)	2848 (w)	2849 (s)	2855 (m)
		2896 (m)	2833 (w)				
ν(COOH)	1739 (vs)	1739 (vw)					
		1702 (m)					
	1689 (sh)	1680 (w)					
	1644 (sh)	1640 (vw)					
$\delta(NH_2)$[b]			1709 (sh)	1707 (vw)		1681 (vw)	
			1675 (sh)	1677 (vw)	1675 (vs)		
			1659 (s)	1659 (vw)		1666 (vw)	
$\nu_{as}(COO)$			1595 (vs)	1601 (vw)	1593 (vs)	1592 (vw)	1597 (vs)
				1585 (vw)			
$\delta(CH_2)$	1465 (s)	1467 (sh)	1473 (m)	1475 (s)		1466 (sh)	
		1456 (sh)		1460 (s)		1458 (sh)	
		1447 (s)	1437 (s)	1447 (s)	1437 (s)	1439 (s)	1440 (s)
		1433 (vs)					
$\nu_s(COO)$	1415 (vs)	1414 (s)	1408 (s)	1417 (s)	1412 (s)	1414 (s)	1409 (s)
			1395 (s)	1405 (s)			
				1397 (s)			
ν[C–$N(CH_2)$]	1125 (w)	1128 (s)	1116 (w)	1118 (m)	1120 (w)	1123 (m)	1121 (m)
ν[C–$N(NH_2)$][b]			1007 (vw)	1007 (vs)	1006 (vw)	1007 (vs)	
ν(C–C)	899 (w)	902 (vs)	928 (m)	933 (vs)	932 (m)	933 (vs)	932 (m)

[a] vs: very strong; s: strong; m: medium; w: weak; vw: very weak; sh: shoulder. [b] Bands derived from the guanidinium cation.

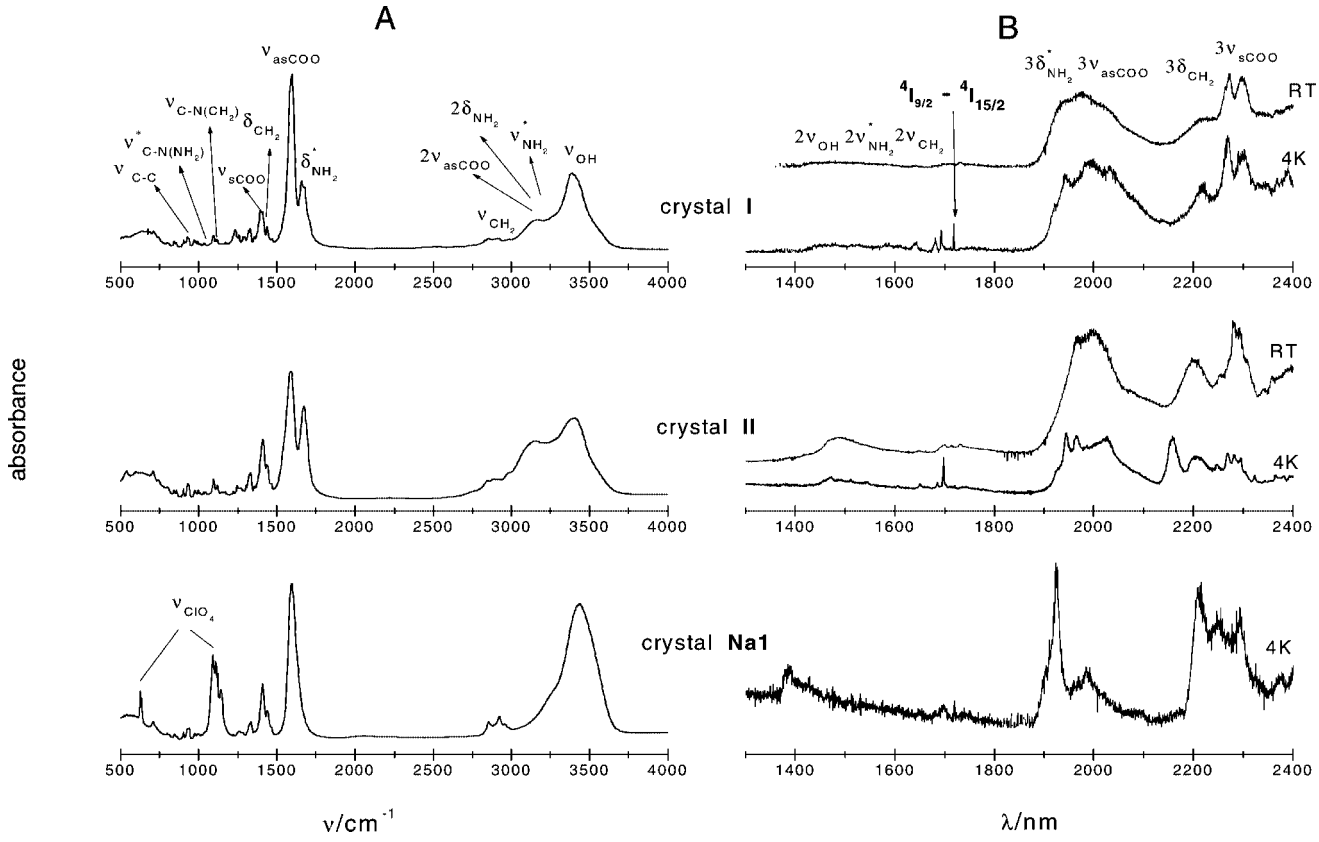

Figure 2. **A** – IR (powder crystals with KBr) and **B** – NIR (single crystals) spectra of Nd^{III}–TTHA complexes in **I**, **II** and **Na1**. Some identified bands are labelled, asterisks respond to bands of the guanidinium cation.

bands strongly dominate the f–f transitions of the Nd^{III} ion in the NIR region and this domination is different for the three non-isomorphic crystals studied.

UV/Vis Spectra of the Nd^{III}–TTHA Complex in Solutions and in Single Crystals

Two transitions in the Nd^{III} absorption spectrum, namely $^4I_{9/2} \rightarrow {}^2P_{1/2}$ and $^4I_{9/2} \rightarrow {}^4G_{5/2}/{}^2G_{7/2}$, are particularly suitable to perform studies of equilibria changes between different species of the Nd^{III}–TTHA complex in solution. The peak positions in the first transition indicate splitting of the ground level in the ligand field of the Nd^{III} environment, whereas the intensity of the hypersensitive $^4I_{9/2} \rightarrow {}^4G_{5/2}/{}^2G_{7/2}$ transition is influenced the most among all the f–f transitions by changes in the immediate surrounding of the Nd^{III} ion.

Analysis of the $^4I_{9/2} \rightarrow {}^2P_{1/2}$ Transition

As can be seen from the equilibria variations between different species for sodium salts of Nd^{III}–TTHA solutions, exemplified by the $^4I_{9/2} \rightarrow {}^2P_{1/2}$ transition in Figure 3, the shape and intensity of these bands do not change further when the pH of the solution exceeds 4. This observation is true for all f–f transitions in spectra of Nd^{III}–TTHA solutions for which the pH was adjusted with either NaOH or $[C(NH_2)_3]_2CO_3$. It can easily be seen from Figure 3 that the number of Stark components in the $^4I_{9/2} \rightarrow {}^2P_{1/2}$ spectra of all studied solutions exceeds five, the number of optical lines predicted by group theory for a single environment of the Nd^{III} ion. This means that for Nd^{III}–TTHA solutions at least two complexes with a different coordination arrangement around the metal ion exist over the entire pH range. At low pH, the peak maximum of the $^4I_{9/2} \rightarrow {}^2P_{1/2}$ transition is at 23248 cm^{-1}, whereas for solutions at pH above 3 it appears at 23310 cm^{-1}. The positions of these peaks correspond to the two different coordination cores of the lanthanide ion found in the previously studied single crystals of the Nd^{III}–TTHA complexes.[8,16] The neodymium entities in those crystals, which were obtained as sodium salts from the same mother liquor at pH 4.5, are $[Nd_2(N_3O_6)_2]^{6-}$ (peak maximum at 23231 cm^{-1})[16] and $[Nd(N_4O_6)]^{3-}$ (peak maximum at 23302 cm^{-1}).[8] From the comparative studies of UV/Vis spectra of single crystals and the solution at pH 7.65 it was proved that the $[Nd(N_3O_6)]^{3-}$ and $[Nd(N_4O_6)]^{3-}$ species are present in this solution in the molar ratio of 1:4.[16] As can be seen from Figure 3, the highest concentration of the first species appears in the solution at a pH below 3, whereas the second species dominates in solution at a pH above 3.5. Hence, one could expect that crystals obtained from solutions in which one of these species prevails will contain this species. Since attempts to obtain crystals from solutions containing sodium cations at very low pH failed, the guanidinium salt solutions were used. The $^4I_{9/2} \rightarrow {}^2P_{1/2}$ spectra of crystals **I** and **II** and solutions from which they were obtained are presented in Fig-

ure 4. Comparing the sodium (Figure 3) and guanidinium (Figure 4) spectra of Nd^{III}–TTHA solutions one can see that a nine-coordinate species with a peak maximum at 23248 cm^{-1} for the sodium solution and 23254 cm^{-1} for the guanidinium solution prevails at a pH below 3. However, the ten-coordinate form is more favoured upon crystallisation in the presence of guanidinium cations. Although the coordination environment of the lanthanide cation is essentially the same in crystals of **I** and **II**, small differences between the bond lengths and angles bring about changes in the position of the $^2P_{1/2}$ state. It is worthwhile noting that the first two peaks in the spectrum of the chiral crystal **II** exactly match the first two peaks of the Nd^{III}–TTHA solution at a pH above 4.

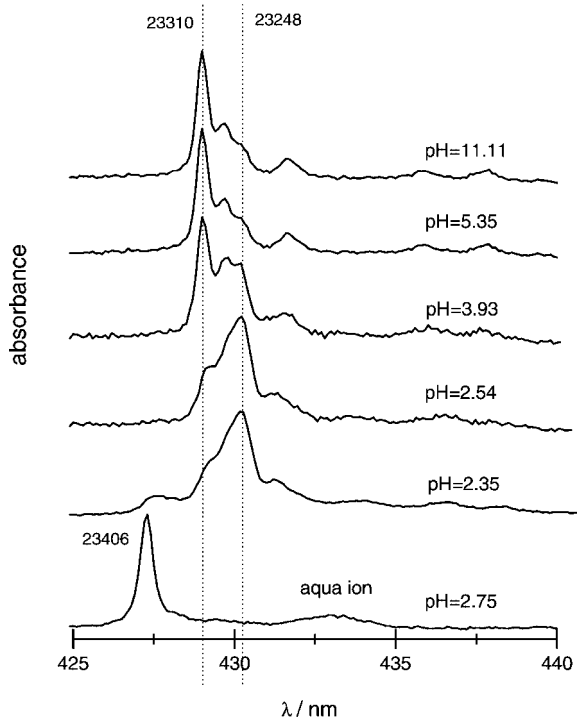

Figure 3. Absorption spectra of the $^4I_{9/2} \rightarrow {}^2P_{1/2}$ transition of the Nd^{III}–TTHA complex in solutions at different pH values adjusted by NaOH (c_{Nd} = 2.219·10^{-2} M, d = 2 cm).

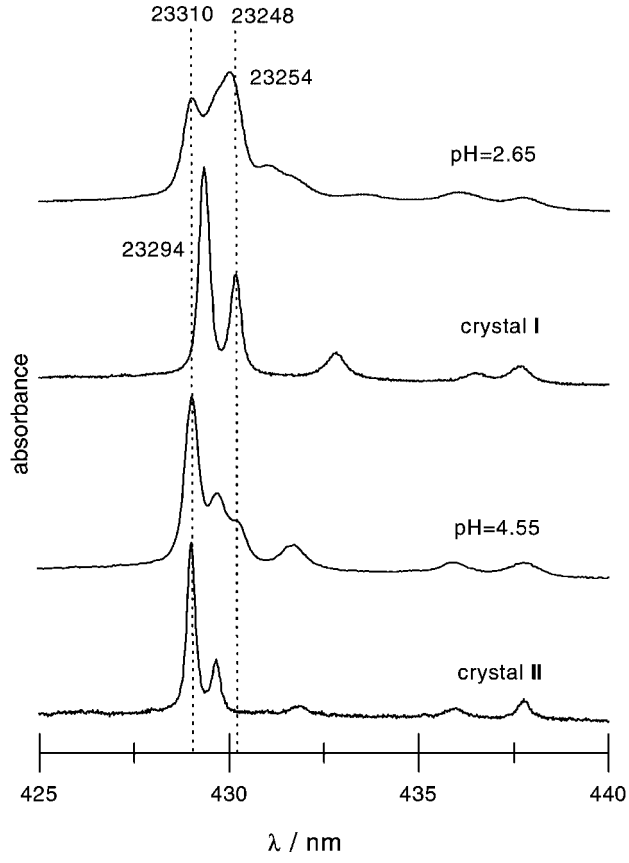

Figure 4. Absorption spectra of the $^4I_{9/2} \rightarrow {}^2P_{1/2}$ transition of guanidinium salts of the Nd^{III}–TTHA complex in solutions and in crystals obtained from these solutions (in solutions: c_{Nd} = 5·10^{-2} M, d = 2 cm; in crystals: c_{Nd} = 2.270 M, d = 0.031 cm for **I** and c_{Nd} = 1.898 M, d = 0.059 cm for **II**).

The positions of the $^4I_{9/2} \rightarrow {}^2P_{1/2}$ peaks and the splittings of the neodymium $^4I_{9/2}$ ground state by the ligand field in the Nd^{III}–TTHA solutions at pH above 4 and in crystals of **Na1**,[8] **Na2**[16] (where **Na2** are crystals of $Na_{0.5}H_{5.5}[Nd_2(TTHA)_2]\cdot 7.5NaClO_4\cdot 16.83H_2O$ with the $[Nd_2(N_3O_6)_2]^{6-}$ core) as well of **I** and **II** are given in Table 3.

As it can be seen from Table 3 and Figure 4, the second intense peak in the $^4I_{9/2} \rightarrow {}^2P_{1/2}$ spectrum of **I** has the same position as the peak that belongs to the $[Nd(N_3O_6)]^{3-}$ species. Therefore, to be sure that the peak at 23248 cm^{-1} in

Table 3. Positions of the $^4I_{9/2} \rightarrow {}^2P_{1/2}$ peaks and the splittings of the neodymium $^4I_{9/2}$ ground state by the ligand field in Nd^{III}–TTHA solutions at pH above 4 and in crystals of **Na1**, **Na2**, **I** and **II**.

Position [cm^{-1}] Solution	Splitting	Position [cm^{-1}] **Na1**	Splitting	Position [cm^{-1}] **Na2**	Splitting	Position [cm^{-1}] **I**	Splitting	Position [cm^{-1}] **II**	Splitting
23310	0	23302	0			23294	0	23310	0
23273	37	23264	38					23273	37
23248	62			23231	0	23248	46		
23165	145	23162	140	23164	67	23106	188	23157	153
22942	368	22946	356	23060	171	22913	381	22937	373
22845	465	22834	468	22899	332	22852	442	22844	466
				22824	407				

solution belongs to the nine-coordinate species, the solution at pH 7.8 (NaOH) was frozen. It was shown previously that only monomeric species exist in solution at this pH value.[6,23] The $^4I_{9/2} \rightarrow {}^2P_{1/2}$ spectrum of this solution, as well as of both sodium and guanidinium crystals recorded at 4 K, are displayed in Figure 5. The spectrum of the frozen solution shows a very intense peak at 23310 cm^{-1} and a very weak shoulder at 23248 cm^{-1}, which confirms the domination of the $[Nd(N_4O_6)]^{3-}$ species over the $[Nd(N_3O_6)]^{3-}$ one and that the peak at 23248 cm^{-1} in the solution indeed represents the nine-coordinate form.

The peak maxima of the deprotonated sodium (**Na1**) as well as guanidinium (**II**) crystals do not shift on cooling the samples down to 4 K, whereas the peak at 23294 cm^{-1} in the spectrum of **I** at room temperature splits into two with energies of 23302 and 23293 cm^{-1} at 4 K. Since in all the spectra of **I** at 4 K there are more lines than would be expected from the relevant multiplicities (J + 1/2), one can assume that a phase transition occurs in **I** below room temperature. This phase transition may also be reflected in the value of the oscillator strength (P) determined at 4 K. The smaller decrease of P in the spectra of crystal **I** than those of crystal **II** at 4 K in comparison with the respective P values determined at room temperature can readily be seen from the P_{exp} results given in Table 4.

It should be pointed out that for crystals of **Na1** and **II**, for which no phase transition is observed, all f–f transitions in the spectra of **Na1** at 4 K are similarly, as can be seen for the $^4I_{9/2} \rightarrow {}^2P_{1/2}$ spectrum, broadened and red-shifted in relation to the spectra of crystal **II**. This may result from vibrational lattice and/or internal ligand modes coupled with the excited levels. This coupling is apparently much weaker for the chiral crystal.

The non-degeneracy of the $^2P_{1/2}$ level means that its shift can be used to study the nephelauxetic effect in neodymium

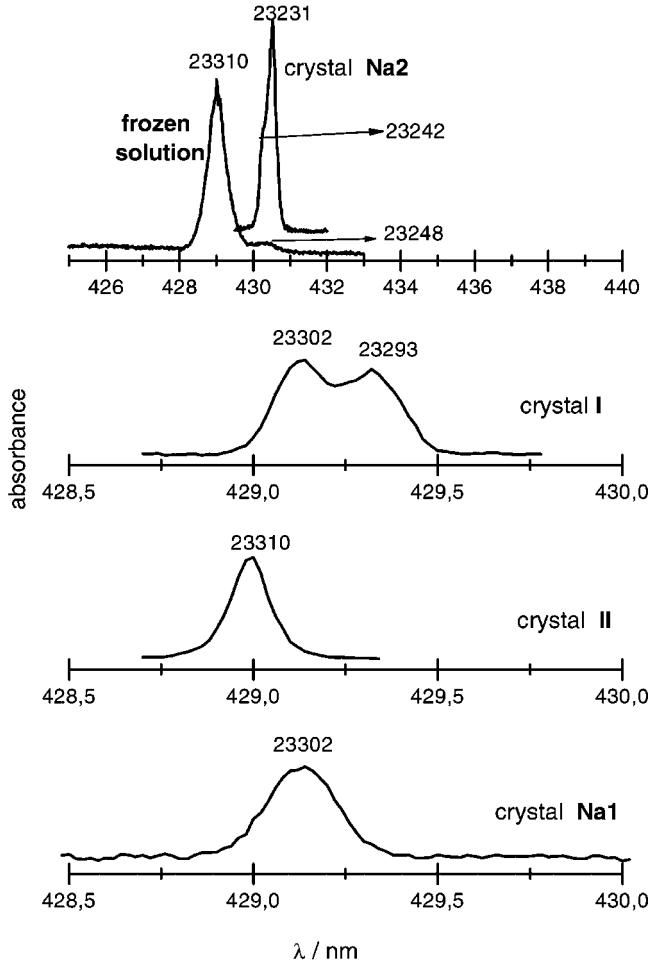

Figure 5. Absorption spectra of the $^4I_{9/2} \rightarrow {}^2P_{1/2}$ transition of the frozen Nd^{III}–TTHA solution with pH 7.8 and crystals of **I**, **II**, **Na1**[8] and **Na2**[16] at 4 K.

Table 4. Oscillator strength values (P_{exp}) and Ω_λ parameters for Nd^{III}–TTHA complexes in solution at different pH values (adjusted by NaOH) and single crystals of **I** and **II**.

	Solution Nd^{III}/TTHA = 1:1.1 c_{Nd} = 2.219 × 10^{-2} M			$[C(NH_2)_3]_2[Nd(HTTHA)]\cdot 3H_2O$ Crystal **I** c_{Nd} = 2.270 M		$[C(NH_2)_3]_3[Nd(TTHA)]\cdot 6H_2O$ Crystal **II** c_{Nd} = 1.898 M	
	pH = 2.45	pH = 5.35	pH = 10.58	293 K	d = 0.031 cm 4 K	293 K	d = 0.059 cm 4 K
Transition(s) $^4I_{9/2} \rightarrow$	10^8P_{exp}	10^8P_{exp}	10^8P_{exp}	10^8P_{exp}	10^8P_{exp}	10^8P_{exp}	10^8P_{exp}
$^4F_{3/2}$	235.55	188.07	233.40	269.20	221.90	207.61	92.01
$^4F_{5/2}$, $^2H_{9/2}$	1079.71	934.61	936.76	886.50	744.21	861.22	459.57
$^4F_{7/2}$, $^4S_{3/2}$	1156.00	1020.77	1030.57	883.18	651.98	913.49	571.49
$^4F_{9/2}$	80.36	79.68	82.92	70.65	44.41	76.27	26.57
$^2H_{11/2}$	20.73	20.31	20.40	15.48	15.59	17.67	10.83
$^4G_{5/2}$, $^2G_{7/2}$	1688.05	1901.53	1935.43	1292.23	860.40	1066.66	588.19
$^2K_{13/2}$, $^4G_{7/2}$, $^4G_{9/2}$	873.72	805.78	809.34	712.30	554.93	695.79	433.97
$^2K_{15/2}$, $^2G_{9/2}$, (^2D, $^2F)_{3/2}$, $^4G_{11/2}$	224.32	207.22	197.55	193.30	234.82	198.87	206.56
$^2P_{1/2}$	36.87	32.2	33.87	39.27	37.92	39.57	16.18
$^2D_{5/2}$	6.10	8.31	9.14	15.39	11.44	13.49	12.05
$^4D_{3/2}$, $^4D_{5/2}$, $^2I_{11/2}$, $^4D_{1/2}$, $^2L_{15/2}$	1118.69	983.68	985.24	1081.66	1011.79	912.33	–
$10^{20}\Omega_2$ [cm^2]	4.06 ± 0.46	5.53 ± 0.47	5.66 ± 0.40	2.10 ± 0.32		1.65 ± 0.36	
$10^{20}\Omega_4$ [cm^2]	5.11 ± 0.43	4.46 ± 0.44	4.48 ± 0.37	4.56 ± 0.30		3.75 ± 0.33	
$10^{20}\Omega_6$ [cm^2]	10.26 ± 0.59	8.91 ± 0.60	9.04 ± 0.52	6.95 ± 0.41		7.22 ± 0.46	
rms·10^7	8.24	8.39	7.24	6.38		7.25	

systems. This effect is interpreted as a covalent contribution to the bonding between the metal ion and the ligands and is connected with metal–ligand distances and coordination numbers.[24] However, a comparison of the structural data given in Table 1 with the spectroscopic data of the $^4I_{9/2} \rightarrow {}^2P_{1/2}$ transition of $[Nd(N_4O_6)]^{3-}$ crystals contradicts this interpretation: of the three $[Nd(N_4O_6)]^{3-}$ crystals, the smallest Nd^{III}–O and Nd^{III}–N distances are found in the sodium crystal, but the spectral results of this crystal do not reflect this in a decrease of the $^2P_{1/2}$ energy level. The $^2P_{1/2}$ energy level shifts, however, agree well with the Δ differences between the ν_{as} and ν_s frequencies of the carboxylate groups. Therefore, our results seem to indicate that the nephelauxetic effect is caused by the change of local polarizability within the inner sphere of the metal ion.

Analysis of the Hypersensitive Transition and f–f Intensities

A comparison of the f–f transitions of all Nd^{III}–TTHA crystals as well as of the solution at pH 5.35, for which there is no difference in the spectra when the pH is adjusted with either NaOH or $[C(NH_2)_3]_2CO_3$, is shown in Figure 6. From the presented spectra, one can see a very good correspondence between the spectra of the monomeric sodium crystal **Na1** of the $[Nd(N_4O_6)]^{3-}$ complex and the solution, in spite of the fact that the presence of 20% of the $[Nd(N_3O_6)]^{3-}$ species was evidenced in the solution.[16] The remarkable similarity of the band shape and the intensities of the most intense f–f transitions between the spectra of the solution and the crystal of **Na1** is not preserved in the case of the protonated crystal **I** or in the deprotonated crystal **II**. For the latter crystal, although the shape of the f–f bands corresponds, to a considerable degree, to that of the solution, the intensity of the $^4I_{9/2} \rightarrow {}^4G_{5/2}/{}^2G_{7/2}$ transition is significantly lower. It is worthwhile stressing that the discussed crystals show low optical anisotropy, as measured by the difference of the intensities of various f–f transitions with different light polarisations and crystal orientations. The intensity results for solutions at different pH values adjusted by NaOH, as well as of crystals of **I** and **II**, are collected in Table 4. An inspection of the oscillator strengths given in this table shows that the largest differences between experimentally determined P values of solutions and crystals occur for the hypersensitive transition. The oscillator strengths of the $^4I_{9/2} \rightarrow {}^4G_{5/2}/{}^2G_{7/2}$ transition of both guanidinium crystals are about two times smaller than those calculated for the solution in which the $[Nd(N_4O_6)]^{3-}$ species dominates. One might suppose that the discrepancies between the P values of the solution and crystals may result from a more symmetrical arrangement of the first coordination sphere in the single crystal. However, this is not the case. In the case of the sodium crystal **Na1**, the $^4I_{9/2} \rightarrow {}^4G_{5/2}/{}^2G_{7/2}$ intensity ($P = 2076.51 \times 10^{-8}$)[8] is higher than that of the solution. Recalculation of the oscillator strengths of the most intense transitions, namely $^4I_{9/2} \rightarrow {}^4G_{5/2}/{}^2G_{7/2}$ (560–600 nm), $^4I_{9/2} \rightarrow {}^4S_{3/2}/{}^4F_{7/2}$ (720–770 nm) and $^4I_{9/2} \rightarrow {}^2H_{9/2}/{}^4F_{5/2}$ (770–830 nm), of the solution at a pH above 4.5 with the P values determined for both **Na1**[8] and **Na2**[16] crystals and the percentage shares of both species reproduces well the oscillator strengths determined experimentally for the solution. This experimental fact is noteworthy, since it can be a helpful indicator of the hypersensitivity mechanism. The small decrease of metal–ligand bond lengths of the crystal **Na1** as compared with

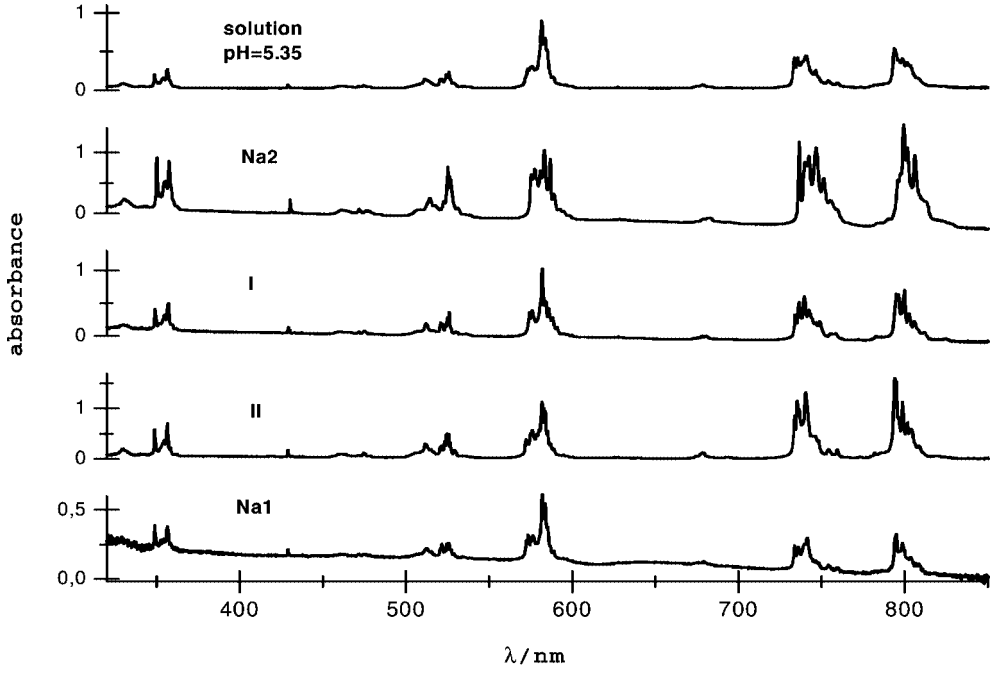

Figure 6. Absorption spectra of f–f transitions of the Nd^{III}–TTHA complex in solution at pH 5.35 (c_{Nd} = 2.219·10^{-2} M, d = 2 cm) and in crystals **Na2** (c_{Nd} = 1.631 M, d = 0.147 cm), **I** (c_{Nd} = 2.270 M, d = 0.031 cm), **II** (c_{Nd} = 1.898 M, d = 0.059 cm) and **Na1** (c_{Nd} = 1.671 M, d = 0.0145 cm).

guanidinium crystals (Table 1) is probably a reason for the intensity enhancement in **Na1**. We also note that somewhat different factors affect the intensities of the hypersensitive transition and the position of the dominant peak in the $^4I_{9/2} \rightarrow {}^2P_{1/2}$ transition discussed above.

Conclusions

Continuing our previous investigations of the structures and spectroscopic properties of complexes of TTHA with lanthanides, we have obtained crystals of two new complexes, namely $[C(NH_2)_3]_2[Nd(HTTHA)]\cdot 3H_2O$ and $[C(NH_2)_3]_3[Nd(TTHA)]\cdot 6H_2O$. The use of different countercations (guanidinium in the present compounds and sodium in our previous reports) has enabled us to observe their role in crystal formation as well as their influence on the spectroscopic properties of the investigated crystals. The complex anions $[Nd(TTHA)]^{3-}$ are monomeric and the neodymium cations are ten-coordinate in both crystals described. Although the coordination environment in both the present complexes is similar to that found in a previously published sodium salt,[8] the oscillator strengths of the hypersensitive transition differ remarkably. This may be attributed to the small differences of the Nd–O and Nd–N bond lengths, which may in turn be induced by networks of H-bonds, strong in the case of guanidinium crystals and competing with the Na–O electrostatic interactions in the case of the sodium crystal.

Experimental Section

Material and Sample Preparation: A stock solution of neodymium perchlorate was prepared from Nd_2O_3 (99.9% Merck). The Nd^{III} concentration was determined complexometrically using xylenol orange as indicator. The stock solution of H_6TTHA (98% Aldrich) was prepared by half-neutralisation with NaOH. The NaOH solution was also used to adjust the pH of the investigated solutions. All measured solutions were prepared with the same ionic strength (0.5 M $NaClO_4$). Crystals of neodymium with the TTHA ligand were prepared by a slightly different method to that described by Ruloff et al.[9] The molar ratio of the applied parent substances of Nd_2O_3, H_6TTHA and $[C(NH_2)_3]_2CO_3$ was 1:2:2. The mixture of substrates was dissolved in water and the pH of the resulting solution was 2.65. This solution was divided into two portions, one of which was basified with guanidinium carbonate to a final pH of 4.55. These solutions of pH 2.65 and 4.55 were left to crystallise and large, well-formed violet crystals of the formula $[C(NH_2)_3]_2[Nd(HTTHA)]\cdot 3H_2O$ and $[C(NH_2)_3]_3[Nd(TTHA)]\cdot 6H_2O$, denoted as **I** (pH 2.65) and **II** (pH 4.55), were obtained. The Nd^{III} concentration in these crystals, determined by ICP, was 2.270 M for **I** and 1.898 M for **II**. **I**: calcd. C 29.71, H 5.20, N 17.33, Nd 17.85; found C 29.23, H 5.45, N 16.87, Nd 19.26. **II**: calcd. C 27.36, H 5.86, N 19.76, Nd 15.66; found C 27.77, H 5.75, N 19.96, Nd 17.11. The density of **I** and **II** was measured by the flotation method in CH_3Cl and CH_3Br and was found to be 1.70 and 1.60 g cm^{-3}, respectively. The refractive index, n, of the crystals was assumed to be 1.50 and that of the measured solutions 1.33.

Crystal Structure Determinations of Complexes I and II: Data for **I** and **II** were collected on a Kuma KM4 diffractometer equipped with a CCD counter. The structures were solved by Patterson methods with SHELXS-97[25] and then refined with SHELXL-97.[26] The C- and N-bonded hydrogen atoms were placed in geometrically calculated positions. All non-H atoms were refined anisotropically. The temperature factors for H-atoms were set as 1.2-times the factors of the C or N atoms to which they are bonded. For **II** the enantiomorph with the better Flack parameter [–0.019(15)] was chosen.

Crystal Data for I: $[C(NH_2)_3]_2[Nd(HTTHA)]\cdot 3H_2O$, $C_{20}H_{43}N_{10}NdO_{15}$, M = 807.88, triclinic, $P\bar{1}$, a = 9.998(2), b = 10.730(2), c = 15.557(3) Å, α = 106.89(3)°, β = 90.27(3)°, γ = 93.24(3)°, V = 1594.0(5) Å^3, Z = 2, T = 293(2) K, μ = 1.711 mm^{-1}, number of reflections measured 11381, number of reflections observed [$I \geq 2\sigma(I)$] 6691, $R(F)$ = 0.0374, $R_w(F^2)$ = 0.0835.

Crystal Data for II: $[C(NH_2)_3]_3[Nd(TTHA)]\cdot 6H_2O$, $C_{21}H_{54}N_{13}NdO_{18}$, M = 921.01, monoclinic, $P2_1$, a = 10.157(2), b = 15.958(3), c = 12.788(3) Å, β = 112.68(3)°, V = 1912.5(7) Å^3, Z = 2, T = 293(2) K, μ = 1.445 mm^{-1}, number of reflections measured 5688, number of reflections observed [$I \geq 2\sigma(I)$] 4837, $R(F)$ = 0.0273, $R_w(F^2)$ = 0.0731.

CCDC-282725 (for **I**) and -282726 (for **II**) contain the supplementary crystallographic data for this paper. These data can be obtained free of charge from The Cambridge Crystallographic Data Centre via www.ccdc.cam.ac.uk/data_request/cif.

Spectroscopic Measurements and Calculations: IR spectra of crystals and H_6TTHA were recorded from KBr pellets on a Bruker FTIR IFS66 spectrometer, while FT-Raman spectra of powder samples were measured on a Bruker RFS 100/S spectrometer with a spectral resolution of 2 cm^{-1}. All electronic absorption spectra were recorded with a Cary 500 UV/Vis/near-IR spectrophotometer which was equipped with an Oxford CF 1204 continuous flow helium cryostat for single crystal measurements at 293 and 4 K.

The intensities of the 4f–4f transitions (P) and values of the Ω_λ parameters were calculated from the Judd–Ofelt[27,28] relation [Equation (1)]:

$$P = \chi \frac{8\pi^2 mc\sigma}{3h(2J+1)} \sum_{\lambda=2,4,6} \Omega_\lambda (f^n \psi J \| U^{(\lambda)} \| f^n \psi' J')^2 \quad (1)$$

where P denotes the oscillator strength, $\chi = (n^2 + 2)^2/9n$ (n is the refractive index), J is the total quantum number of the ground state, $(f^n \psi J \| U^{(\lambda)} \| f^n \psi' J')$ is the reduced matrix element of the respective unit tensor operator $U^{(\lambda)}$, tabulated by Carnall et al.,[29] and Ω_λ is the empirical least-squares-fitted parameter.

Acknowledgments

The authors would like to thank Dr. B. Łydżba-Kopczyńska and Dr. L. Macalik for recording the Raman spectra.

[1] P. Caravan, J. J. Ellison, T. J. McMurry, R. B. Lauffer, *Chem. Rev.* **1999**, *99*, 2293–2352.
[2] S.-B. Yu, A. D. Watson, *Chem. Rev.* **1999**, *99*, 2353–2378.
[3] R. M. Sink, D. C. Buster, A. D. Sherry, *Inorg. Chem.* **1990**, *29*, 3645–3649.
[4] E. F. Gudgin Dickson, A. Pollak, E. P. Diamandis, *J. Photochem. Photobiol. B: Biol.* **1995**, *27*, 3–19.
[5] R. C. Holz, W. DeWitt Horrocks Jr, *Inorg. Chim. Acta* **1990**, *171*, 193–198.

[6] C. A. Chang, H. G. Brittain, J. Telser, M. F. Tweedle, *Inorg. Chem.* **1990**, *29*, 4468–4473.
[7] M. C. Alpoim, A. M. Urbano, C. F. G. C. Geraldes, J. A. Peters, *J. Chem. Soc., Dalton Trans.* **1992**, 463–467.
[8] A. Mondry, P. Starynowicz, *Inorg. Chem.* **1997**, *36*, 1176–1180.
[9] R. Ruloff, P. Prokop, J. Sieler, E. Hoyer, L. Beyer, *Z. Naturforsch., Teil B* **1996**, *51*, 963–968.
[10] R.-Y. Wang, J.-R. Li, T.-Z. Jin, G.-X. Xu, Z.-Y. Zhou, X.-G. Zhou, *Polyhedron* **1997**, *16*, 1361–1364.
[11] R.-Y. Wang, J.-R. Li, T.-Z. Jin, G.-X. Xu, Z.-Y. Zhou, X.-G. Zhou, *Polyhedron* **1997**, *16*, 2037–2040.
[12] R. Ruloff, T. Gelbrich, J. Sieler, E. Hoyer, L. Beyer, *Z. Naturforsch., Teil B* **1997**, *52*, 805–809.
[13] A. Mondry, P. Starynowicz, *New J. Chem.* **2000**, *24*, 603–607.
[14] J. Wang, Z.-R. Liu, X.-D. Zhang, W.-G. Jia, H.-F. Li, *J. Mol. Struct.* **2003**, *644*, 29–36.
[15] D.-F. Chen, W.-C. Yang, R.-Y. Wang, T.-Z. Jin, *Acta Chim. Sin. (Engl. Ed.)* **1997**, *55*, 672–677.
[16] A. Mondry, P. Starynowicz, *J. Chem. Soc., Dalton Trans.* **1998**, 859–863.
[17] A. Mondry, J. P. Riehl, *Acta Phys. Polon. A* **1993**, *84*, 969–974.
[18] C. L. Maupin, A. Mondry, L. Leifer, J. P. Riehl, *J. Phys. Chem. A* **2001**, *105*, 3071–3076.
[19] A. Mondry, S. C. J. Meskers, J. P. Riehl, *J. Lumin.* **1994**, *62*, 17–23.
[20] D. Chapman, D. R. Lloyd, R. H. Prince, *J. Chem. Soc.* **1963**, *85*, 3645–3658.
[21] A. Mondry, K. Bukietyńska, *Molec. Phys.* **2003**, *101*, 923–934.
[22] A. Mondry, K. Bukietyńska, *J. Alloys Compd.* **2004**, *374*, 27–31.
[23] H. G. Brittain, *J. Coord. Chem.* **1990**, *21*, 295–299.
[24] R. D. Peacock, *Struct. Bond.* **1975**, *22*, 83–122.
[25] G. M. Sheldrick, *SHELXS-97, Program for solution of crystal structures*, University of Göttingen, Germany, **1997**.
[26] G. M.Sheldrick, *SHELXL-97*, *Program for refinement of crystal structures*, University of Göttingen, Germany, **1997**.
[27] B. R. Judd, *Phys. Rev.* **1962**, *127*, 750–761.
[28] G. S. Ofelt, *J. Chem. Phys.* **1962**, *37*, 511–520.
[29] W. T. Carnall, P. R. Fields, K. Rajnak, *J. Phys. Chem.* **1968**, *49*, 4424–4442.

Received: November 16, 2005
Published Online: March 16, 2006

